Manipulating Thermal Conductivity via Targeted Phonon Excitation

Xiao Wan[1#], Dongkai Pan[1#], Jing-Tao Lü[2], Nuo Yang[1*]

1. School of Energy and Power Engineering, Huazhong University of Science and Technology, Wuhan 430074, China.
2. School of Physics and Wuhan National High Magnetic Field Center, Huazhong University of Science and Technology, Wuhan 430074, China.

\# X.W. and D. P. contributed equally to this work.

*Corresponding email: nuo@hust.edu.cn (N.Y)

Abstract

Thermal conductivity is a critical property for materials in many practical applications, such as thermoelectric devices and heat dissipation. It has become an issue of great concern that how thermal conductivity can be effectively manipulated. In this work, we manipulate the thermal conductivities of graphene and graphene nanoribbon via targeted phonon quantal excitation. Ab initio calculations show that the thermal conductivity of graphene can be tailored in the range of 45% to 155%, compared with the intrinsic value. Molecular dynamics simulations also exhibit a similar trend (82%-124%) for graphene nanoribbon. This strategy provides a new way for manipulating thermal conductivity in-situ without changing the composition of materials.

Introduction

The manipulation of thermal conductivity holds great importance in applications, such as thermal managements [1-3], and energy devices [4-6]. A deep understanding of phonon scattering mechanism in different heat transfer regimes is critical for modulating thermal conductivity of materials to achieve desirable performances [7-15]. However, manipulating thermal conductivity remains a long-standing challenge in physics and material science, owing to the complex nature of phonon transport.

Recently, the developments in heat conduction help understand the scattering dynamics of heat carriers in nanoscale. Heat conduction can be understood as the propagation of phonons and their scatterings such as phonon-phonon [16-19], impurity [20-22] and boundary scattering [9,23,24]. For phonon-phonon scattering, there are less and weak couplings [25-27] and hydrodynamic phonon transport [11,28] in nanostructures. Impurity scattering is highly frequency dependent and also closely related to the normal process [29], which can redistribute phonon frequencies and control phonon transport by nano-engineering [1,15,20,30,31]. Due to the confinement of size, the phonon transport is largely affected by the boundary scattering [9], resulting in the size dependence of thermal conductivity and the invalid of Fourier's law [32-34].

These progresses have led to new strategies to modulate phonon scattering and thermal conductivities, motivated by the widely demand for thermal management. An enhanced thermal conductivity can be achieved by minimizing phonon–phonon scattering phase space and phonon–impurity scattering in bulk materials [2,14,17-19,35-41]. On the other hand, a reduced thermal conductivity, can be achieved through strategies by increasing phonon scattering [42,43], such as intrinsically increasing anharmonicity or crystal complexity, or extrinsically introducing disorder, defects, boundaries, interfaces and nanoparticles. Besides, the wave nature of phonon [44] can also be utilized to modulate the thermal conductivity, such as nanophononic crystals [45-47], phonon

coherence [48,49] and localization [50-52]. Nevertheless, the strategies mentioned above cannot manipulate thermal conductivity with quantal precision or controllability.

Recently, the targeted phonon mode excitation has been studied in manipulating optical and electrical properties, whose advantages are in situ, flexible, quick response and directness, without modifying original structure. The optical phonons in $MAPbI_3$ can be directly excited by the terahertz excitation pulse and significantly perturb the electron relaxation dynamics [53]. It was also demonstrated experimentally that the performance of an organic optoelectronic system can be modulated by selectively exciting vibrational modes of the molecules [54]. Moreover, the non-equilibrium carrier-phonon dynamics in the photovoltaic system have been discussed in detail for some perovskites. When injecting abundant carriers, the quantal emission of LO phonons, optical phonon decay to acoustic phonons, and other relaxation process have been elaborated in experiment [55-57]. In black phosphorene, the excitation of out-of-plane acoustic phonon can provide strong modulation of the band gap, carrier lifetime and carrier mobility [58]. The excitation of targeted phonons is also used to enhance ion diffusion [59] and induce structural phase transitions [60,61]. The above results provide feasibility for targeted phonon excitation. However, less studies on manipulating thermal conductivity have been performed by mode excitations.

Here, the strategy of quantal exciting phonons is proposed to manipulate thermal conductivity of dielectric materials, where phonons dominate in heat conduction. This strategy excites targeted phonons with an aim to increase/decrease phonon scattering for desired thermal conductivities. Ab initio calculations [62] and molecular dynamical simulations [63] are utilized to demonstrate the effectiveness and capability of the strategy. The graphene and graphene nanoribbon are chosen as the model systems because the thermal conductivities of graphene and its derivatives are well-studied. Our results indicate that thermal conductivity can be manipulated by quantal exciting phonons instead of modifying the structure.

Strategy of Manipulation
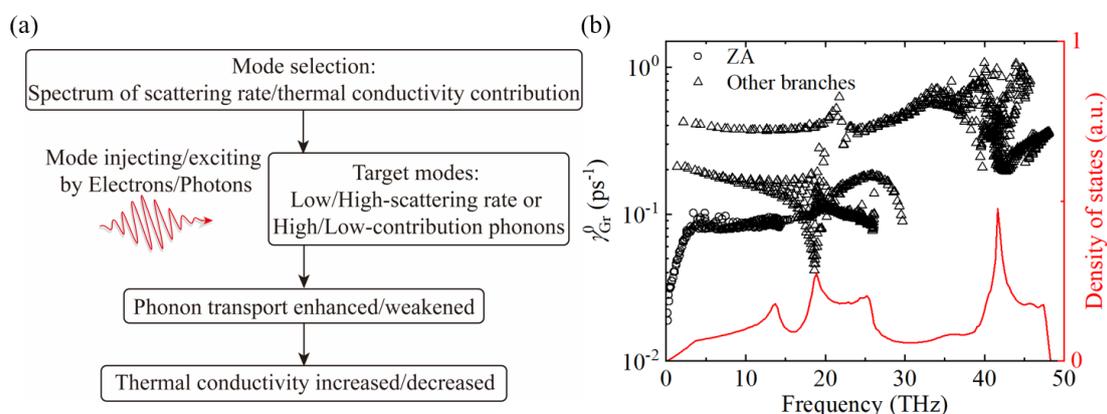
Fig. 1. Manipulating thermal conductivity via targeted phonon excitation. (a) Schematics of manipulation strategy. (b) Density of states (DOS) and intrinsic scattering rates γ_{Gr}^0 of graphene by ab initio calculation, the basis for choosing targeted phonons. The superscript 0 represents the intrinsic value.

The strategy is to manipulate overall thermal conductivity via quantal excitation of targeted phonon modes, as depicted in Fig. 1(a). Firstly, the dominant modes for transport are identified utilizing first principles and molecular dynamics. And then, the energy of these modes is increased artificially. It is the dominant phonons with larger thermal conductivity contribution and weak coupling with others that are excited. Due to these excited new carriers for heat, the thermal conductivity is enhanced. Conversely, when phonons with high scattering rate and relatively low thermal conductivity contribution are excited, it results an enhancement of scatterings and decreasing of thermal conductivity. At the same time, phonon DOS determines the number of the modes excited, thus affecting the effectiveness. It is worth to note that thermal conductivity can be modulated in a wide range by exciting only a few of the dominant phonons, without introducing other scattering mechanism.

The strategy is based on phonon scattering nature in heat conduction. Heat conduction in solids is directly related to phonon scattering, where an individual mode can

participate in various scattering processes. By identifying the characteristic timescale (known as the relaxation time or lifetime), τ, the thermal conductivity can be generally written as an integration as [9,10,23]:

$$\kappa = \frac{1}{3} \int C(\omega) v^2(\omega) \tau(\omega) d\omega \tag{1}$$

where $C(\omega)$ is spectral volumetric specific heat, v is phonon group velocity, and ω is frequency. The diverse scattering can be incorporated into the Matthiessen's rule [9,23]

$$\frac{1}{\tau} = \frac{1}{\tau_{ph-ph}} + \frac{1}{\tau_{im}} + \frac{1}{\tau_b} \tag{2}$$

where τ_{ph-ph}, τ_{im}, and τ_b are the relaxation time due to phonon-phonon, impurity, and boundary scattering processes, respectively. The relaxation time is computed based on Fermi's golden rule [64].

By increasing the energy of targeted phonons, the scattering rate can be changed significantly, leading to the modulation on thermal conductivity. To change the energy of mode n, the phonon occupation numbers are modified for ab initio calculations according to the following formula:

$$E'_n = \hbar\omega_n \frac{N}{e^{\frac{\hbar\omega_n}{k_B T}} - 1} \tag{3}$$

where E'_n is the energy of mode n after modification, $\hbar$ is the reduced Planck constant, k_B is the Boltzmann's constant, T is the lattice temperature and N represents the multiple of energy increase. For molecular dynamics simulations, the atomic velocities are rescaled according to following formula:

$$v'_i = v_i + \frac{1}{\sqrt{m_i}} \left(\sqrt{N} - 1\right) \dot{Q}_n(t) \mathbf{e}_{i,n} \tag{4}$$

where v'_i and v_i are the velocity of atom i after and before modification, respectively, m_i is the atomic mass, $\dot{Q}_n$ is the normal mode velocity coordinate, and $\mathbf{e}_{i,n}$ is the eigenvector. The effectiveness of the strategy is validated in graphene and graphene nanoribbon which have been widely focused. Furthermore, the proposed strategy could be applicable to other low dimensional systems. The ab initio

calculations (Details in Appendix A) for graphene are performed utilizing Vienna ab initio simulation package (VASP) [65]. The phonon transport properties could be obtained by solving the phonon Boltzmann transport equation using ShengBTE packages [66] with the aid of PHONOPY package [67]. Additionally, nonequilibrium molecular dynamics (NEMD, Details in Appendix B) simulations for graphene nanoribbon are conducted using LAMMPS package [68].

Results and Discussions

Firstly, the spectral contribution to intrinsic thermal conductivity of graphene κ_{Gr}^0 is calculated as a guidance on manipulation, as shown in Fig. 2(a). And the iterative solving method is utilized to solve the Boltzmann transport equation accurately. The κ_{Gr}^0 is 3207 W m^{-1} K^{-1} at 300 K, comparable with previous works (1500-4000 W m^{-1} K^{-1}) [69-73]. Fig. 2(a) suggests that the modes at low frequency range dominate the heat conduction in graphene, especially the modes below 5 THz and around 10 THz. Meanwhile, spectral κ_{Gr}^0 drops drastically with frequency going higher, implying a negligible contribution of these modes to heat conduction. This will provide prominent information for further modification.

Then, the energy is injected into those dominant modes for exciting more heat carriers. However, it can be found from Fig. 2(b) that the results do not correspond perfectly to the tendency shown in Fig. 2(a), since the DOS and scattering rates are also essential factors during the modification, as illustrated in Fig. 1(b). DOS indicates the density of modes in a certain frequency interval. Hence, it determines how many modes can be affected during the excitation. Besides, high scattering rate means the modes are strongly scattered. Therefore, higher scattering rate often leads to smaller contribution to heat conduction and larger hindrance to other modes. For graphene, the ZA modes play a much more important role in heat conduction [72], thus the excitation of ZA modes can impose more obvious effects. As a result, the peak of $\kappa_{Gr}/\kappa_{Gr}^0$ locates at around 2 THz, ensuring high enough DOS, low scattering rate as well as high spectral

thermal conductivity. Whereas the trough exists at around 14 THz, near the top of ZA phonon branch, ensuring high enough DOS, relatively high scattering rate and small spectral thermal conductivity compared to other ZA modes.
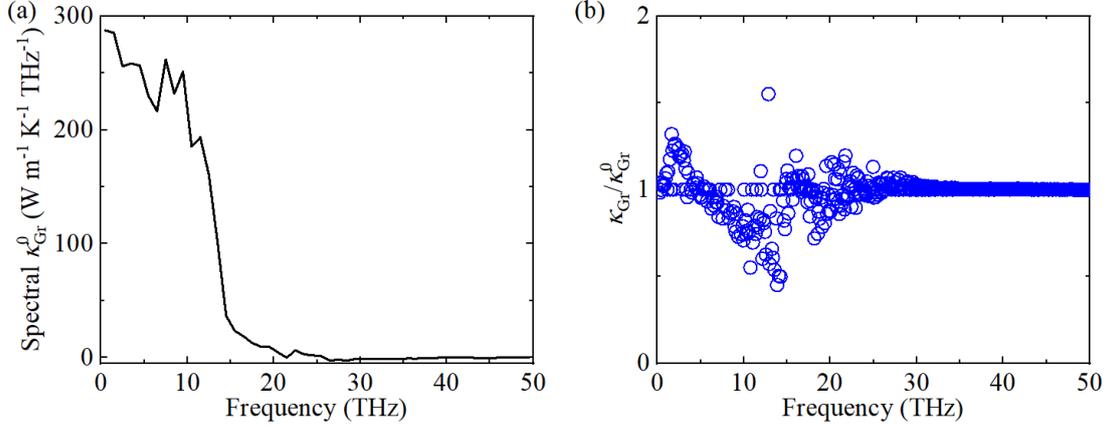
Fig. 2. Thermal conductivity manipulation for graphene via targeted phonon excitation. (a) Spectral contributions to κ_{Gr}^0 as a function of frequency. (b) The relative overall thermal conductivity of graphene after and before the excitation $\kappa_{Gr}/\kappa_{Gr}^0$ as a function of the center frequency for targeted phonons (within 1 THz range). For instance, the first center frequency is 0.5 THz, and the modes in 0-1 THz are excited 10 times larger in energy.

Considering of high-order scatterings, molecular dynamics simulations are performed to validate the feasibility of the modulation strategy. As shown in Fig. 3(a), thermal conductivity contribution spectrum of graphene nanoribbon (24.9×21.6 Å^2) are extracted employing NEMD simulations [74,75]. The intrinsic thermal conductivity of graphene nanoribbon κ_{GNR}^0 is 59.0 W m^{-1} K^{-1} at 300 K, which is consistent with previous study on graphene nanoribbon [46]. Due to the limitation of simulation cell, it has to pick up and excite phonons with smaller wave lengths and higher frequencies (above 6 THz). Moreover, modes around 10 THz show high contribution to overall thermal conductivity in Fig. 3(a). Hence, the modes between 9 and 10 THz are chosen as targeted phonons. The overall thermal conductivity of graphene nanoribbon κ_{GNR} increases by 24.6% (from 59.0 to 73.5 W m^{-1} K^{-1}) when these modes are excited 30

times larger in energy. Fig. 3(a) also shows the thermal conductivity contribution after the excitation. It can be concluded that the increase of κ_{GNR} is mainly contributed from modes below 10 THz, yet the contribution of these models has not changed greatly related to the original values. Furthermore, targeted phonons in other frequency range are excited similarly, as shown in Fig. 3(b). The excitation (30 times larger in energy) of these modes increases the overall thermal conductivity by different ratio (from 10.3% to 24.6%). The modes between 9 and 10 THz show the highest modulation ratio due to high contribution to κ_{GNR}. In general, the enhancement of κ_{GNR} decreases slightly with increasing frequency (over 9 THz), resulting from stronger scattering process of high-frequency modes.
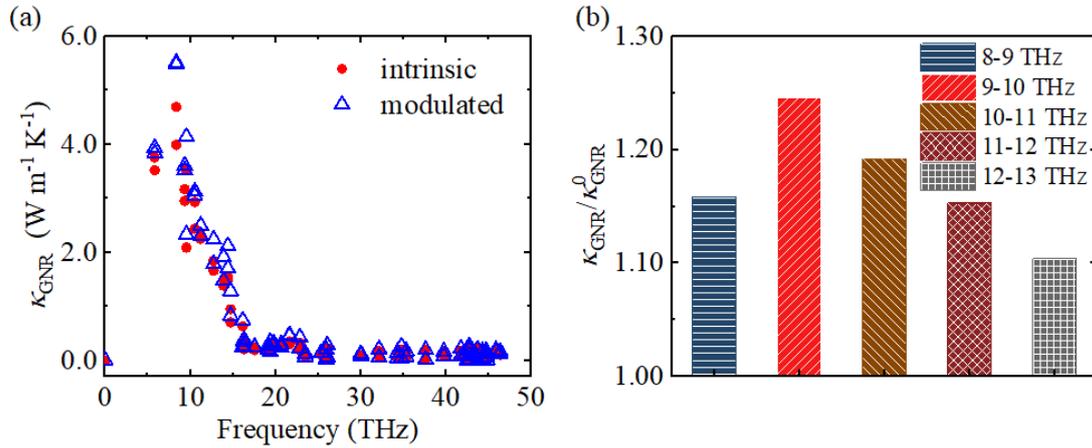
Fig. 3. Thermal conductivity manipulation for graphene nanoribbon via quantal excitation of phonons with high contribution. (a) Thermal conductivity contribution spectrum by molecular dynamics simulations, modes in 9-10 THz are excited 30 times larger in energy. (b) Relative thermal conductivity of graphene nanoribbon after and before the excitation $\kappa_{GNR}/\kappa_{GNR}^{0}$ by exciting different modes utilizing molecular dynamical simulations (30 times larger in energy).

The manipulation results of NEMD simulation for decreasing κ_{GNR} show a similar tendency, compared with ab initio calculations. As shown in Fig. 4(a), modes above 20 THz exhibit low contribution to κ_{GNR}. With the modes between 22 and 23 THz excited 30 times larger in energy, the κ_{GNR} is decreased by 18% (from 59.0 to 48.4 W m^{-1} K^{-}

[1]). The comparison before and after the excitation is also plotted in Fig. 4(a). The contribution of modes to the κ_{GNR} decreases over a wide frequency range. More specifically, the reduction of contribution below 16 THz dominates owing to large original contribution values. Besides, by exciting the modes in other frequencies above 20 THz, the κ_{GNR} also shows a slight reduction (from 5.1% to 18.0%), as illustrated in Fig. 4(b). The reduction of the κ_{GNR} is not significant and has a trend to initially rise and later fall as the frequency of targeted phonons increases. The tendency can be related to the intrinsic scattering rates of modes in different frequency ranges. The modes around 22 THz possess very high scattering rate compared with others.
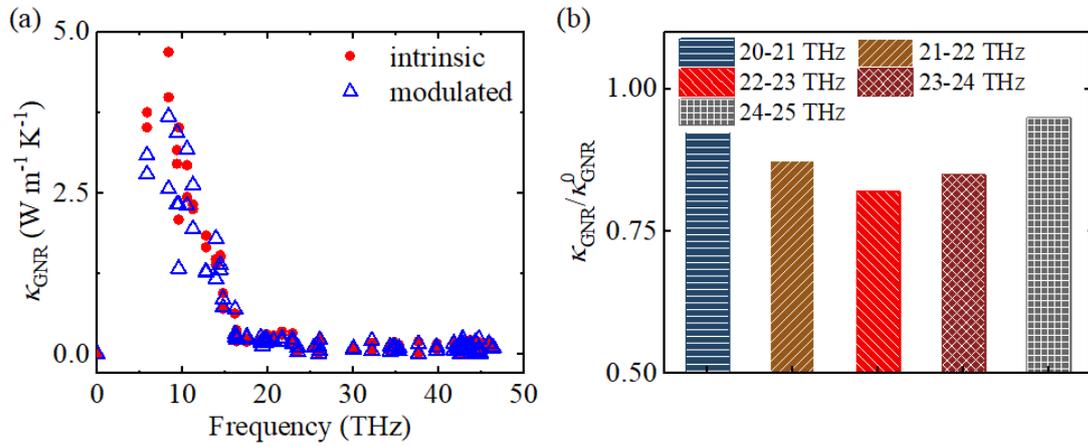
Fig. 4. Thermal conductivity manipulation for graphene nanoribbon via quantal excitation of phonons with strong scattering. (a) Thermal conductivity spectrum by molecular dynamics simulations, modes in 22-23 THz are excited 30 times larger in energy. (b) Relative thermal conductivity of graphene nanoribbon after and before the excitation $\kappa_{GNR}/\kappa_{GNR}^0$ by exciting different modes utilizing molecular dynamical simulations (30 times larger in energy).

Conclusions

In this work, a new strategy for thermal conductivity modulation is presented, which is realized by quantal exciting phonons. The results for the sample structures of graphene and graphene nanoribbon show that the overall thermal conductivity can be modulated

in a wide range via exciting the targeted modes in energy, relative to the intrinsic value. Ab initio calculations and NEMD simulations provide a detailed verification for the modulation. Firstly, the top-contribution or strong-scattering modes are recognized; then, the energy of these modes are increased artificially. It should be emphasized that the idea can be confirmed experimentally. Vibrational mode quantal excitation has been used in manipulating transport properties and inducing structural phase transitions. Furthermore, these findings provide a promising way to manipulate thermal conductivity at mode-level without structure modification and deep insights towards phonon transport in solids.

Acknowledgements

Declaration of Competing Interest

There are no conflicts of interest to declare.

References

[1] X. Qian, J. Zhou, and G. Chen, Nature Materials **20**, 1188 (2021).

[2] C. Huang, X. Qian, and R. Yang, Materials Science and Engineering: R: Reports **132**, 1 (2018).

[3] X. Xu, J. Chen, J. Zhou, and B. Li, Advanced Materials **30**, 1705544 (2018).

[4] J. Mao, G. Chen, and Z. Ren, Nature Materials **20**, 454 (2021).

[5] M. S. Dresselhaus, G. Chen, M. Y. Tang, R. G. Yang, H. Lee, D. Z. Wang, Z. F. Ren, J. P. Fleurial, and P. Gogna, Advanced Materials **19**, 1043 (2007).

[6] D. G. Cahill *et al.*, Applied Physics Reviews **1**, 011305 (2014).

[7] P. B. Allen and J. L. Feldman, Physical Review B **48**, 12581 (1993).

[8] M. T. Dove, *Introduction to Lattice Dynamics* (Cambridge University Press, Cambridge, 1993).

[9] G. Chen, *Nanoscale energy transport and conversion: a parallel treatment of electrons, molecules, phonons, and photons* (Oxford university press, 2005).

[10] C. Kittel, *Introduction to solid state physics* (Wiley, 1996), 7th edn.

[11] G. Chen, Nature Reviews Physics **3**, 555 (2021).

[12] G. Chen, T. Zeng, T. Borca-Tasciuc, and D. Song, Materials Science and Engineering: A **292**, 155 (2000).

[13] N. Li, J. Ren, L. Wang, G. Zhang, P. Hänggi, and B. Li, Reviews of Modern Physics **84**, 1045 (2012).

[14] X. Gu, Y. Wei, X. Yin, B. Li, and R. Yang, Reviews of Modern Physics **90**, 041002 (2018).

[15] Y. Liu *et al.*, Frontiers in Materials **9**, 913764 (2022).

[16] L. Lindsay, D. A. Broido, and T. L. Reinecke, Physical Review Letters **111**, 025901 (2013).

[17] S. Kang Joon, M. Li, H. Wu, H. Nguyen, and Y. Hu, Science **361**, 575 (2018).

[18] S. Li, Q. Zheng, Y. Lv, X. Liu, X. Wang, Y. Huang Pinshane, G. Cahill David, and B. Lv, Science **361**, 579 (2018).

[19] F. Tian *et al.*, Science **361**, 582 (2018).

[20] W. Kim, Journal of Materials Chemistry C **3**, 10336 (2015).

[21] T. Feng, B. Qiu, and X. Ruan, Physical Review B **92**, 235206 (2015).

[22] Z. Liu, J. Mao, T.-H. Liu, G. Chen, and Z. Ren, MRS Bulletin **43**, 181 (2018).

[23] C. L. Tien, *Microscale energy transfer* (CRC Press, 1997).

[24] J. Chen, X. Xu, J. Zhou, and B. Li, Reviews of Modern Physics **94**, 025002 (2022).

[25] M. An, Q. Song, X. Yu, H. Meng, D. Ma, R. Li, Z. Jin, B. Huang, and N. Yang, Nano Letters **17**, 5805 (2017).

[26] C. Deng, Y. Huang, M. An, and N. Yang, Materials Today Physics **16**, 100305 (2021).

[27] D. Pan, Z. Zong, and N. Yang, Acta Physica Sinica **71**, 086302 (2022).

[28] S. Lee, D. Broido, K. Esfarjani, and G. Chen, Nature Communications **6**, 6290 (2015).

[29] J. Callaway, Physical Review **113**, 1046 (1959).

[30] S. Hu, M. An, N. Yang, and B. Li, Nanotechnology **27**, 265702 (2016).

[31] T. Fang, A. Konar, H. Xing, and D. Jena, Physical Review B **78**, 205403 (2008).

[32] N. Yang, G. Zhang, and B. Li, Nano Today **5**, 85 (2010).

[33] Q. Liao, Z. Liu, W. Liu, C. Deng, and N. Yang, Scientific Reports **5**, 16543 (2015).

[34] G. Barbalinardo, Z. Chen, H. Dong, Z. Fan, and D. Donadio, Physical Review Letters **127**, 025902 (2021).

[35] S. Deng, D. Ma, G. Zhang, and N. Yang, Journal of Materials Chemistry A **9**, 24472 (2021).

[36] S. Deng, J. Yuan, Y. Lin, X. Yu, D. Ma, Y. Huang, R. Ji, G. Zhang, and N. Yang, Nano Energy **82**, 105749 (2021).

[37] X. Yu, D. Ma, C. Deng, X. Wan, M. An, H. Meng, X. Li, X. Huang, and N. Yang, Chinese Physics Letters **38**, 014401 (2021).

[38] C. Dames, Science **361**, 549 (2018).

[39] A. van Roekeghem, J. Carrete, C. Oses, S. Curtarolo, and N. Mingo, Physical Review X **6**, 041061 (2016).

[40] A. Henry and G. Chen, Physical Review Letters **101**, 235502 (2008).

[41] S. Shen, A. Henry, J. Tong, R. Zheng, and G. Chen, Nature Nanotechnology **5**, 251 (2010).

[42] A. Katre, J. Carrete, B. Dongre, G. K. H. Madsen, and N. Mingo, Physical Review Letters **119**, 075902 (2017).

[43] M. Yamawaki, M. Ohnishi, S. Ju, and J. Shiomi, Science Advances **4**, eaar4192 (2018).

[44] D. Ma, A. Arora, S. Deng, G. Xie, J. Shiomi, and N. Yang, Materials Today Physics **8**, 56 (2019).

[45] L. Yang, N. Yang, and B. Li, Nano Letters **14**, 1734 (2014).

[46] D. Ma, X. Wan, and N. Yang, Physical Review B **98**, 245420 (2018).

[47] M. I. Hussein, C.-N. Tsai, and H. Honarvar, Advanced Functional Materials **30**, 1906718 (2020).

[48] X. Wan, D. Ma, D. Pan, L. Yang, and N. Yang, Materials Today Physics **20**, 100445 (2021).

[49] Z. Zhang, Y. Guo, M. Bescond, J. Chen, M. Nomura, and S. Volz, Physical Review Letters **128**, 015901 (2022).

[50] D. Ma, H. Ding, H. Meng, L. Feng, Y. Wu, J. Shiomi, and N. Yang, Physical Review B **94**, 165434 (2016).

[51] B. L. Davis and M. I. Hussein, Physical Review Letters **112**, 055505 (2014).

[52] X. Zheng and B. Li, arXiv:2201.00251 (2022).

[53] F. Sekiguchi, H. Hirori, G. Yumoto, A. Shimazaki, T. Nakamura, A. Wakamiya, and Y. Kanemitsu, Physical Review Letters **126**, 077401 (2021).

[54] A. A. Bakulin *et al.*, Nature Communications **6**, 7880 (2015).

[55] M. B. Price *et al.*, Nature Communications **6**, 8420 (2015).

[56] Y. Yang, D. P. Ostrowski, R. M. France, K. Zhu, J. van de Lagemaat, J. M. Luther, and M. C. Beard, Nature Photonics **10**, 53 (2016).

[57] J. Yang *et al.*, Nature Communications **8**, 14120 (2017).

[58] H. Guo, W. Chu, O. V. Prezhdo, Q. Zheng, and J. Zhao, The Journal of Physical Chemistry Letters **12**, 3960 (2021).

[59] K. Gordiz, S. Muy, W. G. Zeier, Y. Shao-Horn, and A. Henry, Cell Reports Physical Science **2**, 100431 (2021).

[60] A. P. Itin and M. I. Katsnelson, Physical Review B **97**, 184304 (2018).

[61] M. Hase, P. Fons, K. Mitrofanov, A. V. Kolobov, and J. Tominaga, Nature Communications **6**, 8367 (2015).

[62] A. Ward, D. A. Broido, D. A. Stewart, and G. Deinzer, Physical Review B **80**, 125203 (2009).

[63] D. C. Rapaport, *The Art of Molecular Dynamics Simulation* (Cambridge University Press, Cambridge, 2004), 2 edn.

[64] J. M. Ziman, *Electrons and phonons: the theory of transport phenomena in solids* (Oxford university press, 2001).

[65] G. Kresse and J. Furthmüller, Physical Review B **54**, 11169 (1996).

[66] W. Li, J. Carrete, N. A. Katcho, and N. Mingo, Computer Physics Communications **185**, 1747

(2014).

[67] A. Togo, F. Oba, and I. Tanaka, Physical Review B **78**, 134106 (2008).

[68] S. Plimpton, Journal of Computational Physics **117**, 1 (1995).

[69] A. A. Balandin, Nature Materials **10**, 569 (2011).

[70] A. A. Balandin, S. Ghosh, W. Bao, I. Calizo, D. Teweldebrhan, F. Miao, and C. N. Lau, Nano Letters **8**, 902 (2008).

[71] W. Cai, A. L. Moore, Y. Zhu, X. Li, S. Chen, L. Shi, and R. S. Ruoff, Nano Letters **10**, 1645 (2010).

[72] L. Lindsay, W. Li, J. Carrete, N. Mingo, D. A. Broido, and T. L. Reinecke, Physical Review B **89**, 155426 (2014).

[73] X. Xu *et al.*, Nature Communications **5**, 3689 (2014).

[74] Y. Zhou and M. Hu, Physical Review B **92**, 195205 (2015).

[75] Y. Zhou, X. Zhang, and M. Hu, Physical Review B **92**, 195204 (2015).